Effects of biochar-based silicate fertilizer on iron reduction by bacteria and root iron plaque formation in subtropical paddy soils

Meifen Lin[a#], Xiaotong Wang[a#], Josep Peñuelas[b,c], Jordi Sardans[b,c], Abdulwahed Fahad Alrefaei[d], Yi Zheng[a,*], Xuping Xu[a,*], Qiang Jin[e,f], Xuyang Liu[e,f], Weiqi Wang[e,f,*]

[a] *College of Life Science, Fujian Normal University, Fuzhou, 350108, China*

[b] *CSIC, Global Ecology Unit CREAF-CSIC-UAB, 08913 Bellaterra, Catalonia, Spain*

[c] *CREAF, 08913 Cerdanyola del Vallès, Catalonia, Spain*

[d] *Department of Zoology, College of Science, King Saud University, P.O. Box 2455, Riyadh 11451, Saudi Arabia*

[e] *Key Laboratory of Humid Subtropical Eco-Geographical Process, Ministry of Education, Fujian Normal University, Fuzhou, 350007, China*

[f] *College of Geographical Sciences, Fujian Normal University, Fuzhou, 350007, China*

***Corresponding author.**

Yi Zheng: College of Life Science, Fujian Normal University, Keji Street #1, Minhou County, Fuzhou, 350108, China. E-mail addresses: eyizheng@fjnu.edu.cn (Y. Zheng).

Xuping Xu: College of Life Science, Fujian Normal University, Keji Street #1, Minhou County, Fuzhou, 350108, China. E-mail addresses: xuping@fjnu.edu.cn (X. Xu).

Weiqi Wang: College of Geographical Sciences, Fujian Normal University, Shangsan Street #8, Cangshan District, Fuzhou, 350007, China. E-mail addresses: wangweiqi15@163.com (W. Wang).

#These authors contributed equally to this work.

Abstract

Purpose Biochar and silicate-enriched steel-slag, as agricultural and industrial waste materials, are used to improve soil physicochemical properties and soil fertility; however, there are few studies on the effects of their combined application to paddy fields on the formation of root Fe plaque.

Materials and methods We tested the effects of four application rates (0, 300, 600 and 900 kg ha^{-1}) of biochar-based silicate fertilizer (BSF) to early and late rice on root Fe plaque formation.

Results and discussion Application of BSF increased soil total carbon and total nitrogen concentrations in late rice, and total phosphorus concentrations were increased by 47.03% at the jointing stage and 27.73% at the mature growth stage of early rice following application of BSF at 600 kg ha^{-1}, respectively. The three application treatments all significantly increased the abundance of soil IRB in late rice, and application of 600 kg of BSF ha^{-1} increased IRB abundance by 52.16% and 66.59% at the jointing and mature growth stage, respectively. Both IRB abundance and IP concentration were positively correlated with Fe(II) and negatively correlated with Fe(III) in late rice. There were positive correlation between soil Fe(II) concentrations and water content, and negative correlation with Fe(III).

Conclusions Our study demonstrated that moderate inputs of BSF (600 kg ha^{-1}) increased soil Fe reduction and subsequently promoted the formation of more soluble Fe^{2+} and iron plaque formation through soil fluidity and Fe^{2+} movement to roots**.** We suggest that the application of BSF to dry-wet rice paddies may contribute to reduction in agricultural pollution, improvement in soil conditions, and the production of sustainable healthy food crops.

Keywords Paddy soils · Iron reduction · Iron plaque · Biochar-based silicate fertilizer

1. Introduction

In China, management and control of point source pollution associated with rapid economic development have been effective; however, limitation of non-point source (diffuse) pollution has been less successful and is of particular concern in agricultural systems (Wang et al. 2021; Yao 2020). For example, the overuse of agrochemical fertilizer and inappropriate ratios of nitrogen (N) to phosphorus (P) lead to eutrophication and acidification of soils that cause soil hardening and declines in crop productivity, and threaten the ecology of non-crop plants and aquatic systems, such as rivers (Soltangheisi et al. 2018). Thus, combined improvements in fertilizer utilization rates by crop plants and reductions in fertilizer application rates will lead to declines in non-point source pollution of agroecosystems due to lower levels of leached N and P to soils and water courses.

Globally, China is key producer of rice, with 27% of its arable land under paddy cultivation (China Statistical Yearbook 2018), in which alternate dry-wet soil management creates phased anaerobic and aerobic conditions and associated redox reaction cycles (Kögel-Knabner et al. 2010; Lovley et al. 2004). In anaerobic sediments of flooded paddy fields, iron-reducing bacteria (IRB) use ferric ion, Fe(III), as a respiratory chain terminal electron acceptor, with organic matter or H_2 as an electron donor, to generate ferrous ion, Fe(II), in this important soil biogeochemical process (Amos et al. 2007; Lovley and Chapelle 1995; Sung et al. 2006). Studies have shown that the application of biochar to soils provides suitable environmental conditions for the survival of IRB (Lehmann et al.

2003; Topoliantz et al. 2005) and the concomitant increase in soil organic carbon (C) content serves as an "electron shuttle body" that accelerates the extracellular electron transport function between IRB and iron oxides and promotes Fe(III) reduction, leading to increases in soil accumulations of Fe(II) (Weber et al. 2006). While studies of biochar tend to focus on its impacts on microorganisms and iron reduction, less is known about its role in the formation of a red-brown film (iron plaque, IP) at the surface of plant roots from the deposition of crystalline and amorphous iron oxides or hydroxides under waterlogged conditions. In flooded paddy fields, for example, iron (Fe) plaque affects the absorption and accumulation of beneficial and polluting elements, thereby impacting the nutritional value and safety of rice as a major food staple (Liu et al. 2009). Fe plaque is believed to form on roots when large amounts of Fe(II) present in the growth medium are locally oxidized to Fe(III), through the release of excess oxygen to the rhizosphere by roots, and while it is known that biochar promotes the reduction of Fe(III) and increases accumulations of the highly soluble Fe(II) in the rhizosphere, effects of its addition to paddy soils on the formation of Fe plaque on rice plant roots remain unclear.

The treatment and reuse of industrial and agricultural waste is increasingly important in the context of sustainable development. Biochar is created from agricultural and forestry waste material and tends to be alkaline, so its application to agricultural production systems impacts levels of soil pH (Glaser et al. 2002; Laird et al. 2010a), while its high levels of porosity and specific surface area enhance the adsorption capacity of water and nutrient elements (Liang et al. 2006) and improve soil fertility, nutrient uptake, and crop yields (Bu and Xue 2014; Glaser et al. 2002; Liang et al. 2006; Van et al. 2010). However, the low density of biochar increases its soil mobility, particularly under wet conditions, so biochar-based silicate fertilizer (BSF), which is a granular compound comprising biochar and silicate enriched steel slag, has been developed to reduce losses of biochar amendment from agricultural soils. Although application of BSF is known to reduce emission fluxes of greenhouse gases, due to effects on microbe community structure and associated Fe redox processes (Lin et al. 2021; Wang et al. 2017; Wang et al. 2019), understanding of impacts on Fe metabolism and the formation of Fe plaque in paddy soils is limited, but may be important for the reduction of agricultural pollution and improvement in rice safety.

Here, we studied the effects of contrasting rates of BSF application to rice paddies on soil nutrient content, Fe metabolism, IRB, plant root Fe plaque formation, and the internal relationships between soil Fe metabolism, bacteria, and iron plaque formation to test the hypotheses that BSF 1) absorbs nutrient elements and reduces N and P losses; 2) improves IRB growth and reproduction; 3) indirectly promotes Fe plaque formation on the surface of rice roots; and, 4) drives the relationship between soil Fe metabolism, IRB and Fe plaque formation.

2. Materials and methods

2.1. Study site

The study site was a 7-ha paddy field at the Wufeng Comprehensive Experimental Base of the Rice Research Institute (26.1°N, 119.3°E), Fujian, China, where the climate is subtropical monsoon (Wang et al. 2014); during the study period, mean air temperature was c. 19.6 ºC and mean annual precipitation was c. 1,393 mm. The paddy field was managed following local agronomic practice, based on a rotation of early rice-late rice-vegetable; the traditional irrigation method of waterlogging was adopted during the early growth stages of rice, and after the tillering stage, the field was waterlogged, drained, and re-irrigated (Ma et al. 2012). The experimental paddy field was manually leveled prior to crop planting, to ensure soil uniformity.

2.2. Experimental design and treatments

The field experiment comprised three replicates of three rates of BSF (300, 600 and 900 kg ha^{-1}), plus an untreated control, applied to 10-m^2 plots that were arranged in a randomized complete block; the plots were separated using PVC boards (30 × 30 × 30 cm). Cultivation of early rice (Hesheng 10) and late rice (Jiafuzhan) was from 18 April to 6 July, 2018 and 1 August to 8 November, 2018, respectively, and standard fertilizers (compound fertilizer: N:P_2O_5:K_2O=16:16:16%; urea: 46% N) were applied 1 day before transplantation (42 kg N ha^{-1}, 40 kg P_2O_5 ha^{-1}, and 40 kg K_2O ha^{-1}), about 1 week after transplantation, at the tillering stage (35 kg N ha^{-1}, 20 kg P_2O_5 ha^{-1}, and 20 kg K_2O ha^{-1}), and about 8 weeks after transplantation, at the panicle stage (18 kg N ha^{-1}, 10 kg P_2O_5 ha^{-1}, and 10 kg K_2O ha^{-1}). The main elements of BSF (pH 8.93 ± 0.03; Taigang Harsco Technology Co., Ltd.) comprised C (5.54%), N (0.52%), P (0.48%), K (0.53%), Ca (16%), Mg (2.81%), Fe (0.78%), S (0.21%) and Si (14%).

2.3. Soil and plant sampling and analysis

We collected soil and plant samples at the jointing and mature growth stages of the early (2 June and 6 July, 2018, respectively) and late rice (19 September and 8 November, 2018, respectively). Three replicate samples of soil (0-15 cm) were collected, using a small soil sampler, and combined to form a single composite sample per plot; after stones and plant roots had been removed, the sampled soils were placed in an ice box and taken to the laboratory for analysis. Meanwhile, rice with roughly the same growth and height was selected in the area where the soil was sampled. The plants were carefully removed from the soils and placed in bags separately.

The soil samples were divided into two, where soil microorganisms were analyzed from fresh soil and soil physicochemical properties were analyzed from air dried, ground, and screened soil. The rice plant samples were rinsed with tap water to remove soil from root material; then, the roots were rinsed twice with deionized water and subsequently immersed in deionized water, prior to analysis within 24 h.

2.3.1. Soil physicochemical properties

Soil total carbon (TC) and total nitrogen (TN) concentrations were determined using an elemental analyzer (Elementar Vario Max, Elementar Scientific Instruments, Hanau, Germany), and soil total phosphorus (TP) concentration was determined using perchloric acid digestion and ammonium-molybdate colorimetry in a continuous flow analyzer (SKALAR SAN++, Netherlands). Stoichiometric ratios (C:N, C:P, and N:P) in soil were calculated as mass ratio. Total Fe (TFe) concentration of non-rhizosphere soil was determined by digesting the fresh soils with 1 M HCl solution; ferrous ions were extracted using 1,10-phenanthroline and the concentration of the extracted solution was determined using UV spectrophotometry (He and Qu 2008; Wang et al. 2016), while ferric ion concentration was calculated by subtracting ferrous ion concentrations from total Fe concentrations. Soil pH was measured using a pH/temperature meter (IQ Scientific Instruments, Carlsbad, USA) with a soil to water ratio of 1:5 (w/v), electrical conductivity (EC) was measured using a 2265FS EC meter (Spectrum Technologies Inc., Paxinos, USA), and water content (WC) was measured as the difference in mass of soil before and after drying at 105 °C to a constant weight; soil bulk density (BD) was measured using the ring knife method (Lu 2000).

2.3.2. Iron-reducing bacteria

Abundance and community composition of IRB were measured from 5 g of fresh soil that was weighed into a triangular flask containing 45 mL of sterile ultra-pure water. The soil suspension (concentration of 10^{-1}) was oscillated for 10 min and then diluted at intervals of 10^{-2}-10^{-7}; next, 1 mL of the last five dilutions was inoculated into a test tube containing IRB culture solution, and each dilution was repeated three times; blank tube of non-inoculated sample was used as a control. The dilutions (inoculated and non-inoculated) were incubated in the test tubes at 30 ℃ for 10 d, when the culture solution was observed for a change in color from yellow-green to light green or colorless, indicating presence of IRB (Lin et al. 2021). A quantity index value for IRB abundance, which was based on the number of IRB-positive test tubes at the various dilutions, was used to determine the approximation value of the number of IRB. The approximation value was multiplied by the dilution factor to derive the most probable number (MPN) of IRB (Lin 2010).

Genomic IRB DNA was extracted from soil samples using the cetyltrimethylammonium bromide method, and purity and concentration of DNA were detected using agarose gel electrophoresis. Then, the extracted DNA was diluted with sterile water to 1 ng μL^{-1} and used as template for PCR amplification using specific primers for the 16S V3-V4 region, (341F: CCT AYG GGR BGC ASC AG; and 806R: GGA CTA CNN GGG TAT CTA AT), and high-fidelity enzymes. Amplified PCR products were purified using a PCR clean-up kit (Thermo Scientific, Shanghai, China) and stored at -20 °C prior to analysis.

Effects of treatment on IRB species abundance and community composition were based on clustering analysis (97% consistency) of operational taxonomic units (OTUs) in UPARSE, using the QIIME (V. 1.9.1) and Mothur (V. 1.36.1) to filter original DNA sequences and remove chimera to obtain optimized sequences (Caporaso et al. 2010). Representative sequences were those with the highest OTU occurrence frequency, and species annotation analysis on OTUs (threshold set at 0.8-1) was conducted using the Mothur method and SILVA132's SSUrRNA database (Edgar 2013).

2.3.3. Iron plaque

Iron plaque concentration on the surface of rice plant roots was analyzed using the dithionite-citrate-bicarbonate method (Gao et al. 2007; Hu et al. 2020; Wan et al. 2020). Fresh rice plant roots were immersed in a solution of 40 mL of 0.3 mol L^{-1} sodium citrate ($Na_3C_6H_5O_7 \cdot 2H_2O$) and 5 mL of 1 mol L^{-1} sodium bicarbonate ($NaHCO_3$, pH=9) for 10 min, to which 1 g of sodium dithionite ($Na_2S_2O_4$) was added and shaken at 280 r min^{-1} and 25 ºC 3 h; then, the extraction solution was filtered through a 0.22-µm microporous filter membrane into a 100-mL volumetric flask. After extraction, the rice roots were washed three times using ultra-pure water that was collected in a volumetric flask and increased to 100-mL using additional ultra-pure water; the washed roots were dried at 75 ºC to a constant weight and weighed. Concentration of Fe in the extraction solution was determined using UV spectrophotometer and the amount of iron plaque on the root surface was expressed as mg g^{-1} of dry root.

2.4. Statistical analysis

Main effects of treatment were tested using one-way analysis of variance (ANOVA) at $p<0.05$ and between treatment means were compared using least significant differences ($LSD_{0.05}$), unless stated otherwise. Pearson correlation analysis was used to test the association between soil physicochemical properties (e.g. pH, EC, WC, BD, TC, TN, TP, C:N, C:P, and N:P) and iron concentration (e.g. TFe, Fe(II), Fe(III), IRB, and IP) in early and late rice under different BSF treatments. Statistical analyses were conducted in SPSS version 23.0 (IBM, Armonk, NY, USA) (Xue 2013). We used principal components analysis (PCA) in the ade4 and ggplot2 packages of R software version 2.15.3 (R Core Team 2018; Chen 2014) to visualize treatment differences in microbe community structure, based on OTUs.

3. Results

3.1. Effects of BSF on soil C, N, P concentrations

There were within-growth stage effects of rate of BSF on soil TC, TN, and TP concentrations in early and late rice and within-treatment rate differences between growth stages within a season (Fig. 1). While there were no effects of BSF on soil TC at the jointing or mature stages of early rice or at the jointing stage in late rice, its addition led to greater soil TC concentrations at the mature growth stage of late rice, regardless of application rate (p<0.05). When BSF was applied at 300 and 600 kg ha^{-1} to early rice, soil TC content was greater at the mature growth stage than at the jointing stage (p<0.05).

While there were no effects of BSF on soil TN concentrations at the jointing or mature growth stages of early rice, its addition led to greater levels of soil TN content at the jointing stage of late rice, regardless of application rate, and greater levels of soil TN concentration at the mature growth stage of late rice when applied at 300 and 900 kg ha^{-1} (p<0.05). Application of 300 kg ha^{-1} of BSF to early and late rice led to greater soil TN concentrations at the mature growth stage than at the jointing stage, and application of BSF at 900 kg ha^{-1} to late rice led to greater soil TN concentration at the mature growth stage than at the jointing stage (p<0.05).

There were variable, within-growth stage effects of rate of BSF on soil TP concentrations. In early rice, the soil TP concentration in the application of 600 kg ha^{-1} was greater than that in the untreated control during the jointing and mature growth stages. In late rice, levels of soil TP concentration at the jointing stage were greatest when BSF was applied at 900 kg ha^{-1} and lowest when BSF was applied at 300 and 600 kg ha^{-1} (p<0.05), while application of BSF at 600 and 900 kg ha^{-1} reduced levels of soil TP concentration at the mature growth stage (p<0.05). There were within-treatment rate differences in effects of BSF between growth stages when it was applied at 900 kg ha^{-1}, where levels of soil TP were greater at the mature stage of early rice and jointing stage of late rice (p<0.05).

3.2. Effects of BSF on soil C, N, P stoichiometry

There was a strong positive correlation between soil concentration of TC, TN and TP (p<0.01; Fig. 2), where the association between TN and TC (R^2=0.662) was greater than between TC and TP (R^2=0.493) and TN and TP (R^2=0.191) and we found within-growth stage effects of rate of BSF on soil TC, TN and TP stoichiometry in early and late rice and within-treatment rate differences between growth stages within a season (Fig. 3). While there were no differences in soil C:N ratios in early rice, ratios were lowest at the mature growth stage in late rice, when BSF was applied at 900 kg ha^{-1} and ratios were greater at the jointing stage of late rice than at the mature stage in the untreated control and when BSF was applied at 300 and 900 kg ha^{-1} (p<0.05). There were no within-treatment rate differences in soil C:P or N:P ratios between growth stages within a season; however, in early rice

C:P and N:P ratios were lowest at the jointing stage in the 600 kg of BSF ha^{-1} treatment and highest at the mature growth stage in the 300 kg of BSF ha^{-1} treatment (p<0.05), and in late rice, ratios were highest at the jointing stage in the 300 kg of BSF ha^{-1} treatment and highest at the mature growth stage in the 600 kg of BSF ha^{-1} treatment (p<0.05).

3.3. Effects of BSF on soil Fe concentrations

There were within-growth stage effects of rate of BSF on soil total Fe, Fe(III) and Fe(II) concentrations in early and late rice and within-treatment rate differences between growth stages within a season (Fig. 4). While there were no effects of treatment on total Fe content at the jointing and mature growth stages in early rice, concentration in late rice was greater at the jointing stage when BSF was applied at 600 kg ha^{-1} and at the mature growth stage, regardless of application rate (p<0.05). Soil total Fe concentration in early and late rice was greater in the untreated control at the jointing stage than at the mature growth stage (p<0.05).

Soil concentrations of Fe(III) at the jointing stage of early rice were greatest when BSF was applied at 900 kg ha^{-1} and lowest when BSF was applied at 600 kg ha^{-1}, while in late rice, concentrations at the jointing growth stage were greatest when BSF was applied at 600 kg ha^{-1}; concentrations at the mature growth stage of late rice were increased by the addition of BSF, and were greatest under 600 kg of BSF ha^{-1} (p<0.05). In early rice, soil Fe(III) concentration was lower at the mature growth stage in the absence of BSF and when it was applied at 900 kg ha^{-1}, while in late rice concentration was consistently lower at the jointing stage, regardless of application of BSF (p<0.05).

Soil concentrations of Fe(II) in early rice were greater at the jointing stage when BSF was applied at 600 kg ha^{-1} (p<0.05); there were no effects of treatment at the mature growth stage of early rice or at either growth stage of late rice. In early rice, concentrations of Fe(II) were lower at the mature growth stage than at jointing stage when BSF was applied at 300 and 600 kg ha^{-1} (p<0.05), while in late rice, concentrations were consistently lower at the mature growth stage, regardless of application of BSF (p<0.05).

3.4. Effects of BSF on root Fe plaque

Content of Fe plaque on the surface of rice roots was affected by application of BSF and there were between growth stage differences in content within a treatment (Fig. 5). While there were no treatment effects on Fe plaque content at the jointing stages of early and late rice, content at the mature growth stage was greater when BSF was applied at 600 and 900 kg ha^{-1} to early rice and 600 kg ha^{-1} to late rice (p<0.05). Root Fe plaque content was lower at the mature growth stage than at jointing stage in the absence of BSF in early and late rice and when BSF was applied at 600 kg ha^{-1} to early rice and at 300 kg ha^{-1} to late rice (p<0.05).

3.5. Effects of BSF on soil IRB

There were treatment effects on the abundance of soil IRB at both growth stages of early and late rice and within-treatments in the two rice cropping seasons (Fig. 6). In early rice, soil IRB were more abundant at the jointing growth stage when BSF was applied at 300 and 600 kg ha^{-1} and least abundant in the 900 kg of BSF ha^{-1} treatment (p<0.05); soil IRB abundance was reduced by the 300 and 900 kg of BSF ha^{-1} treatment at the mature growth stage (p<0.05). In late rice, no matter which application treatment was compared with the untreated control, the abundance of soil IRB was significantly increased, and application of 600 kg of BSF ha^{-1} increased IRB abundance by 52.16% and 66.59% at the jointing and mature growth stage, respectively. In early and late rice, abundance of IRB within a treatment was consistently lower at the mature growth stage than at jointing (p<0.05).

Analysis of treatment effects on soil IRB community structure at the jointing stage of early and late rice (Fig. 7a) showed that principal components (PCs) 1 and 2 accounted for 43.79% of the variation in community composition; communities under addition of 300 and 600 kg of BSF ha^{-1} to late and early rice, respectively, were similar to each other along PC2 and dissimilar from each other along PC1 and from the other communities along both PCs. Analysis of treatment effects on soil IRB community structure at the mature growth stage of early and late rice (Fig. 7b) showed that PCs 1 and 2 accounted for 55.99% of the variation in community composition, where communities of the control in late rice and 300 kg of BSF ha^{-1} treatments in early and late rice clustered along the two PCs, as did those of the 600 and 900 kg of BSF ha^{-1} treatments.

3.6. Association between soil physicochemical properties and iron metabolism

Across the treatments, we found associations among and between levels of soil physicochemical properties, IRB, and root Fe plaque (Fig. 8). In early rice, there were positive correlations between soil Fe(II) concentrations and water content (WC), electrical conductivity (EC), pH (p<0.01), and negative correlations with bulk density (BD), TC, and TN (p<0.01). IRB abundances were positively correlated with Fe(II) , WC, EC, and pH (p<0.01) and negatively correlated with BD, TC, and TN (p<0.01); iron plaque (IP) concentrations were positively correlated with WC, pH, Fe(II), and IRB (p<0.01), and negatively correlated with TC and TN (p<0.05) (Fig. 8a).

In late rice (Fig. 8b), soil Fe(II) concentrations were positively correlated with WC and EC ($p<0.01$), and negatively correlated with BD ($p<0.01$). There were positive correlations between soil Fe(III) concentrations and BD, TN ($p<0.01$), and negative correlations with WC and TFe ($p<0.05$). Both IRB abundance and IP concentration were positively correlated with Fe(II) and negatively correlated with Fe(III) ($p<0.01$).

4. Discussion

4.1. Soil Fe reduction and IRB community structure

The low density and porous structure of biochar creates suitable habitat conditions for Fe-reducing microorganisms that lead to increases in their abundance and activity (Lehmann et al. 2003; Topoliantz et al. 2005), leading to increased reduction of Fe(III) to Fe(II). Our results showed that changes in Fe(III) concentration in late rice contrasted with those for Fe(II), while IRB abundance was positively associated with soil Fe(II) content and negatively associated with soil Fe(III) content, likely due to flooded soil conditions at the jointing growth stage and when soil IRB abundance was higher than that at the mature growth stage. We found that application of BSF increased soil C concentrations and improved conditions for the reduction of Fe(III) by IRB to Fe(II), while at the mature growth stage of both early and late rice, when levels of soil WC and associated abundance and activity of anaerobic microorganisms decreased, activity of aerobic microbes promoted the oxidation of soil Fe(II) that led to an increase in soil Fe(III) concentrations.

Our study showed differences in effects of BSF application rate between growth stage and rice season on paddy IRB community structure, and the effect of 600 kg of BSF ha^{-1} application amount is the most significant. Changes in soil microbe community structure are triggered by several factors, including soil type, pH, temperature and humidity, and crop root exudates, tillage methods, and climate conditions (Pan et al. 2019). Soils at the study site tend to be acidic (Chen et al. 2014) and the addition of BSF, which contains weak alkaline substances, such as SiO_2, CaO and MgO, increased levels of pH of the study soils. Our results showed that paddy soil pH and Fe(II) concentrations were positively associated, supporting the findings of Wu et al. (2014) and Jia (2017) who found that initially alkaline paddy soils tended to impede Fe(III) reduction, whereas initially acid soils tended to facilitate Fe(III) reduction (Wu et al. 2014), and changes in paddy soil pH that affected Fe(III) reduction processes also impacted soil microbe community structure (Jia 2017). Therefore, the appropriate application of BSF (600 kg ha^{-1}) to paddy soils can provide suitable microhabitat conditions for IRB to a large extent, and improve the soil pH through the action of biochar.

4.2. Formation of root Fe plaque

The formation of root Fe plaque is the product of Fe(II) oxidation when iron oxide or hydroxide is produced during waterlogging of the dry-wet management cycles of paddy rice production (Liu et al. 2014; Yang et al. 2018; Zandi et al. 2021). We found that the amount of root Fe plaque of early and late rice at the jointing stage tended to be greater than at the mature growth stage, due to contrasting flooded and drained conditions, respectively. Rice plants adapt to flooded conditions by forming aeration tissue to transport atmospheric oxygen to the root system through the leaves and stems and carry exocrine oxygen from the root system to the rhizosphere; this response forms a local oxidation environment at the root surface (Liu et al. 2009). Our results showed that the application of BSF (600 and 900 kg ha^{-1}) tended to increase soil Fe plaque content, because it increased availability of nutrients for soil IRB that led to increased levels of soil Fe(III) reduction to Fe(II) by microorganisms; Fe(II) was then rapidly transported to rice roots, due to its high levels of solubility of Fe(II) and soil fluidity, where it was subsequently oxidized to Fe(III) and promoted the formation of root Fe plaque. Studies have found that the addition of biochar increases aerenchyma formation and porosity in calamus (*Acorus calamus* L.) roots (Huang et al. 2019), and according to this study, we suggest future research should test whether the application of BSF similarly improves the aerenchyma oxygen transport and root oxygen production in rice plants.

Fe plaque may act as a "reservoir" for binding and retaining nutrients as well as a "barrier" to the absorption of elements (Zhang et al. 2020), because it has been shown to reduce the accumulation of heavy metal elements, such as Cd, Cr and As, in plants and protect plants from effects of heavy metal toxicity (Li et al. 2015; Li et al. 2019; Zhou et al. 2018). Zhang et al. (2020) found that intensification of Fe(II) concentrations increases the content of Fe plaque on *Spartina alterniflora* roots, while concurrently enhancing resistance to effects of artificial sewage; similarly, our study showed that the amount of root Fe plaque in early and late rice was positively associated with Fe(II) concentrations.

Christensen et al. (1998) showed that large amounts of root Fe plaque adsorb soluble phosphate in solution to form the Fe-P compound, leading to 20 to 260-fold increases in P concentrations of root Fe plaque and 25 to 1100-fold decreases in P concentrations in water that alleviate levels of water eutrophication. Similarly, Liang et al. (2006) found that rice root Fe plaque strongly absorbed P and this capacity, which was positively associated with soil Fe(II) concentrations, improved overall rice plant P absorption. We found that P concentrations were lower in late rice than in early rice, possibly due to P absorption by rice root Fe plaque and microorganisms, and although application of BSF increased soil nutrient availability, limiting nutrients, such as P, may have led to increased competition for, and absorption and consumption of soil P among and between microorganisms and plants in late rice.

4.3. Variation in soil nutrients

Essential nutrient elements for plant growth and development comprise C, N, and P (Ma and Wang 2011) and biochar, which is rich in C, has high chemical and biological stability that may inhibit the mineralization of soil organic C and promote the formation of humus, leading to increased levels of soil organic matter (Chen et al. 2015; Laird et al. 2009; Zwieten et al. 2010). The application of BSF mixed granulation of biochar and steel slag led to increased soil TC concentrations in late rice, consistent with previous studies (Chen et al. 2015). Xu (2018) reported that high soil concentrations of C provide sufficient capacity for soil N fixation and absorption and improve soil C:N ratios that are more stable than C:P and N:P ratios, due to similar and near-synchronous C and N responses to changes in environmental factors (Li et al. 2015); these responses by C and N were reflected in our experiment, and supported by their positive association. We found that soil TN concentrations of late rice were higher in the BSF-treated soils and soil TP concentrations were increased by 47.03% at the jointing stage and 27.73% at the mature growth stage of early rice following application of BSF at 600 kg ha^{-1}, respectively, as a result of effects of BSF on soil N and P concentrations that include biochar absorbs soil nutrients and reduces losses of N and P (Ali et al. 2008; Gao et al. 2021), due to its porous structure and large specific surface area (Farrell et al. 2014; Olmo et al. 2016; Wu et al. 2018). It is also possible that biochar and steel slag have strong adsorption capacity on soil N and P through cation exchange (Wu et al. 2018), and slowly release part of nutrient elements for plant absorption and utilization under the interaction with the soil ecological environment (Laird et al. 2010b). For example, Laird et al. (2010b) found that wood-based biochar applied to an indoor soil column at 20 g kg^{-1} reduced leaching losses of N and P by 11% and 69%, respectively, while Chen et al. (2019) showed that addition of biochar reduced soil TN and TP losses, thereby increasing soil fertility.

The ratio of soil C:N:P indicates the availability of nutrients and reflects soil element cycling and balance, including under the influence of environmental factors, and the ratio of C:P reflects the retention effect of soil microorganisms on P. Research has shown that higher C:P ratios indicate lower soil P concentrations and a weak ability of microorganisms to retain P, and lower C:P ratios indicate relatively high soil P concentrations and strong ability of microorganisms to retain (Qiao 2020). Indeed, we found that C:P ratios in late rice were higher than in early rice, while soil P concentrations in late rice were lower than early rice, possibly due to contrasting soil microbial activity between the rice seasons (Neubauer et al. 2005; Xu et al. 2019). In this study, early rice was cultivated in spring and summer, when temperatures increase, along with production of rice metabolites and root exudates; the addition of BSF, which improves environmental conditions for microorganisms, likely enhanced the P retention ability of microorganisms. In contrast, late rice was cultivated in autumn and winter, when there was a decrease in temperature and production of rice metabolites and root exudates; during this time, the rate of Fe reduction and microbial activity reduced, so the P retention ability of microorganisms similarly reduced.

4.4. Relationships between Fe plaque formation, Fe(III) reduction, and IRB

Iron in soils tends to exist as an oxide and the re-accumulation of weathered parent material during soil formation processes is a key global contributor of iron oxide in soils (Wang et al. 2018). Iron oxide minerals formed during weathering of carbonate rocks are initially occupy micropores, in the form of colloids, or are adsorbed on the surface of clay minerals, in the form of amorphous iron oxide film. Under continuous weathering, iron oxide colloids interact with each other and with clay minerals on the coagulation and activation of iron oxide colloid and during transfer and re-precipitation to eventually form iron oxide. Due to the dry-wet management cycles of rice, paddy soils contain large amounts of Fe(III) oxide that provides suitable environment conditions for nutrient recycling and iron redox (Kögel-Knabner et al. 2010), and application of BSF provides further input of abundant nutrients and microhabitat conditions for microorganisms. When paddy soils are flooded and anaerobic, IRB use organic matter or H_2 as electron donors and Fe(III) as an electron acceptor to reduce Fe(III) to Fe(II) through the electron transfer process (Chen et al. 2016); concurrent re-oxidation of Fe(II) to Fe(III) provides conditions for the formation of root Fe plaque (Deng et al. 2019); indeed, we found that the amount of Fe plaque was positively associated with soil Fe(II) concentrations and IRB abundance. Rice plants increased the amount of aerenchyma in response to flooding conditions and obtained oxygen through root and microorganism oxidation products (Li et al. 2019; Liu et al. 2015); when excess oxygen was secreted into the rhizosphere, iron-oxidizing bacteria oxidize Fe(II) to Fe(III), forming oxides or hydroxides that then accumulate on the surface of rice roots as Fe plaque (Yu et al. 2016).

5. Conclusion

Our study demonstrated that application of BSF (600 and 900 kg ha^{-1}) to paddy soils absorbed nutrient elements and reduced losses of N and P in early and late rice.

The three application treatments all significantly increased the abundance of soil IRB in late rice, and application of 600 kg of BSF ha^{-1} increased IRB abundance by 52.16% and 66.59% at the jointing and mature growth stage, respectively.

We found that both IRB abundance and IP concentration were positively correlated with Fe(II) and negatively correlated with Fe(III) in late rice. In summary, the application of BSF promoted Fe(III) reduction by IRB that led to increased accumulation of Fe(II) and its transport to rice roots, and subsequent precipitation of Fe(III) in the rhizosphere and formation of root Fe plaque.

Overall, we suggest that moderate inputs of BSF (600 kg ha^{-1}) to dry-wet rice paddies may contribute to reduction in agricultural non-point source pollution, improvement in soil conditions, and the production of sustainable healthy food crops.

Acknowledgments

The authors would like to thank Xinfu Lan, Youyang Chen, Xiaoxuan Chen for their assistance with field sampling and laboratory analysis.

Author contribution

Conceptualization	ML, WW
Methodology	ML, XW, YZ, XX, QJ, XL, WW,
Software	ML, XW, YZ, XX, QJ, XL, WW, JP, JS
Validation	WW, ML, JS,

Formal analysis	WW, ML, JS
Investigation	ML, XW, YZ, XX, QJ, XL, WW
Resources	ML, XW, YZ, XX, QJ, XL, WW
Data Curation	ML, WW, JS
Writing - Original Draft	WW, ML, JS
Writing - Review & Editing	ML, XW, JP, JS, YZ, XX, QJ, XL, WW
Visualization	ML, JS, WW
Supervision	WW, JP, JS
Project administration	WW, JP
Funding acquisition	WW, JP, JS

Funding Information

Funding was provided by the National Natural Science Foundation of China (42077086; 41901111), the Natural Science Foundation of Fujian Province (2020J01188; 2021J06019). JP and JS were funded by Spanish Government projects PID2019-110521GB-I00 and PID2020115770RB-I, Fundación Ramón Areces project ELEMENTAL-CLIMATE, and Catalan government project SGR2017-1005. We extend our appreciation to the Researchers Supporting Project (no. RSP-2021/218), King Saud University, Riyadh, Saudi Arabia.

Declarations

Conflict of interest The authors declare no competing interests.

References

Ali MA, Lee CH, Kim PJ (2008) Effect of silicate fertilizer on reducing methane emission during rice cultivation. Biol Fert Soils 44:597-604

Amos BK, Sung Y, Fletcher KE, Gentry TJ, Wu WM, Criddle CS et al (2007) Detection and quantification of *Geobacter lovleyi* strain SZ: implications for bioremediation at tetrachloroethene and uranium-impacted sites. Appl Environ Microbiol 73:6898-6904

Bu XL, Xue JH (2014) Biochar effects on soil habitat and plant growth: A review. Ecol Environ Sci 23:535-540

Caporaso JG, Kuczynski J, Stombaugh J, Bittinger K, Bushman FD, Costello EK et al (2010) QIIME allows analysis of high-throughput community sequencing data. Nat Methods 7:335-336

Chen JX (2014) Applied statistics using R. Dongbei University of Finance & Economics Press

Chen L, Zhang HX, Li Y, Zheng SL, Liu FH (2016) The role of microorganisms in the geochemical iron cycle. Sci Sin (Vitae) 46:1069-1078

Chen QH, Xu Z, Tang JC, Jin WB, Sun ZG, Lu BL (2019) Influences of adding biochar on loss of nitrogen and phosphorus and yield of rape in soil. J Agric Sci Technol 21:130-137

Chen SL, Li JW, Deng HM (2014) The relationship between physical and chemical properties of soil and heavy metal content in Fujian coastal farmland. Hubei Agric Sci 53:3025-3029

Chen W, Hu XY, Lu HN (2015) Impacts of biochar input on mineralization of native soil organic carbon. Environ Sci 36:2300-2305

Christensen KK, Jensen HS, Andersen FS, Holmer M, Wigand C (1998) Interferences between root plaque formation and phosphorus availability for isoetids in sediments of oligotrophic lakes. Biogeochemistry 43:107-128

Deng LW, Wang LJ, Wang YL, Li W, Ma JT, Zhang LY et al (2019) Formation mechanism of iron plaque of rice: research progress. Chin Agric Sci Bull 35:1-5

Edgar RC (2013) UPARSE: highly accurate OTU sequences from microbial amplicon reads. Nat Methods 10:996-998

Farrell M, Macdonald LM, Butler G, Valle IC, Condron LM (2014) Biochar and fertiliser applications influence phosphorus fractionation and wheat yield. Biol Fert Soils 50:169-178

Gao LY, Lin WP, Zhang FJ, Zhou QY, Liu SM, Xiong M et al (2021) Research progress of biochar in improving soil acidification. Guangdong Agricul Sci 48:35-44

Gao MX, Hu ZY, Wang GD (2007) The extraction and elemental analysis of iron plaque from the surface of rice root. Environ Chem 26:331-334

Glaser B, Lehmann J, Zech W (2002) Ameliorating physical and chemical properties of highly weathered soils in the tropics with charcoal-a review. Biol Fert Soils 35:219-230

He JZ, Qu D (2008) Dissimilatory Fe(Ⅲ) reduction characteristics of paddy soil extract cultures treated with glucose or fatty acids. J Environ Sci 20:1103-1108

Hu LQ, Zeng M, Lei M, Liao BH, Zhou H (2020) Effect of zero-valent iron on arsenic uptake by rice (*Oryza sativa* L.) and its relationship with iron, arsenic, and phosphorus in soil and iron plaque. Water, Air, & Soil Pollut 231:262-272

Huang L, Liang YK, Liang Y, Luo X, Chen YC (2019) Influences of biochar application on root aerenchyma and radial oxygen loss of *Acorus calamus* in relation to subsurface flow in a constructed wetland. Environ Sci 40:1280-1286

Jia R (2017) Contribution of microbial fermentation to iron(Ⅲ) reduction in submerged paddy soils. Xianyang: Northwest Agriculture and Forestry University

Kögel-Knabner I, Amelung W, Cao ZH, Fiedler S, Frenzel P, Jahn R et al (2010) Biogeochemistry of paddy soils. Geoderma 157:1-14

Laird DA, Brown RC, Amonette JE, Lehmann J (2009) Review of the pyrolysis platform for coproducing bio-oil and biochar. Biofuels Bioprod Bioref 3:547-562

Laird DA, Fleming P, Davis DD, Horton R, Wang BQ, Karlen DL (2010a) Impact of biochar amendment on the quality of a typical Midwestern agricultural soil. Geoderma 158:443-449

Laird DA, Fleming P, Wang BQ, Horton R, Karlen D (2010b) Biochar impact on nutrient leaching from a Midwestern agricultural soil. Geoderma 158:436-442

Lehmann J, Da Silva JP, Steiner C, Steiner C, Nehls T, Zech W, Glaser B (2003) Nutrient availability and leaching in an archaeological Anthrosol and a Ferralsol of the Central Amazon basin: fertilizer, manure and charcoal amendments. Plant Soil 249:343-357

Li HL, Gong L, Zhu ML, Liu ZY, Xie LN, Hong Y (2015) Stoichiometric characteristics of soil in an oasis on northern edge of Tarim Basin. China, Acta Pedol Sin 52:1345-1355

Li RY, Zhou ZG, Xu XH, Xie XJ, Zhang Q, Liu YC (2019) Effects of silicon application on uptake of arsenic and phosphorus and formation of iron plaque in rice seedlings grown in an arsenic-contaminated soil. Bull. Bull Environ Contam and Toxicol 103:133-139

Li RY, Zhou ZG, Zhang YH, Xie XJ, Li YX, Shen XH (2015) Uptake and accumulation characteristics of arsenic and iron plaque in rice at different growth stages. Commun Soil Sci Plan 46:2509-2522

Li TT, Feng YF, Zhu A, Huang J, Wang H, Li SY et al (2019) Effects of main water-saving irrigation methods on morphological and physiological traits of rice roots. Chin J Rice Sci 33:293-302

Liang B, Lehmann J, Solomon D, Kinyang J, Grossman J, O'Neill B et al (2006) Black carbon increases cation exchange capacity in soils. Soil Sci Soc Am J 70:1719-1730

Liang Y, Zhu YG, Xia Y, Li Z, Ma Y (2006) Iron plaque enhances phosphorus uptake by rice (*Oryza sativa*) growing under varying phosphorus and iron concentrations. Ann Appl Biol 149:305-312

Lin MF, Zheng Y, Wang XT, Xu XP, Wang WQ (2021) Effects of carbon-enriched silicon fertilizer on the community characteristics of iron-reducing bacteria in paddy fields. China Environ Sci 41:1778-1789

Lin XG (2010) Principles and methods of soil microbiology research. Higher Education Press, Beijing (In Chinese)

Liu CY, Chen CL, Gong XF, Zhou WB, Yang JY (2014) Progress in research of iron plaque on root surface of wetland plants. Acta Ecol Sin 34:2470-2480

Liu HJ, Zhang JL, Han XR, Zhang FS (2009) Influences of iron plaque on element uptake by plants and its affecting factors. Soils 41:335-343

Liu YY, Fu ZQ, Long WF, Zhong J, Du QX (2015) Study on the effect of morphological variation of root aerenchyma on the ability of root radial oxygen loss in rice. Res Agric Modern 36:1105-1111

Lovley DR, Chapelle FH (1995) Deep subsurface microbial processes. Rev Geophys 33:365-381

Lovley DR, Holmes DE, Nevin KP (2004) Dissimilatory Fe(III) and Mn(IV) reduction. Adv Microb Physiol 49:219-286

Lu RK (2000) Soil agricultural chemical analysis method. China Agricultural Science and Technology Press, Beijing (In Chinese)

Ma YY, Tong C, Wang WQ, Zeng CS (2012) Effect of azolla on CH_4 and N_2O emissions in Fuzhou Plain paddy fields. Chin J Eco Agric 20:723-727

Ma YY, Wang WQ (2011) Carbon, nitrogen and phosphorus content and the ecological stoichiometric ratios of paddy field soil-plants in Minjiang River estuary. Subtrop Agric Res 7:182-187

National Bureau of Statistics of the People's Republic of China (2018) China statistical yearbook. China Statistics Press, Beijing (In Chinese)

Neubauer SC, Givler K, Valentine S, Megonigal JP (2005) Seasonal patterns and plant-mediated controls of subsurface wetland biogeochemistry. Ecology 86:3334-3344

Olmo M, Villar R, Salazar P, Alburquerque JA (2016) Changes in soil nutrient availability explain biochar's impact on wheat root development. Plant Soil 399:333-343

Pan XC, Tang HM, Xiao XP, Li C, Tang WG, Wang K et al (2019) Paddy soil microbial diversity under tillage practices: research progress. Chin Agric Sci Bull 35:51-57

Qiao Y (2020) Soil C-N-P stoichiometric characteristics and influencing factors in subtropical evergreen broad-leaved forests. Shanghai: East China Normal University

R Core Team (2018) R: A Language and Environment for Statistical Computing, 3.5 ed

Soltangheisi A, Rodrigues M, Coelho MJA, Gasperini AM, Sartor LR, Pavinato PS (2018) Changes in soil phosphorus lability promoted by phosphate sources and cover crops. Soil Till Res 179:20-28

Sung Y, Fletcher KE, Ritalahti KM, Apkarian RP, Ramos HN, Sanford RA et al (2006) *Geobacter lovleyi* sp. nov. strain SZ, a novel metal-reducing and tetrachloroethene-dechlorinating bacterium. Appl Environ Microbiol 72:2775-2782

Topoliantz S, Ponge JF, Ballof S (2005) Manioc peel and charcoal: a potential organic amendment for sustainable soil fertility in the tropics. Biol Fert Soils 41:15-21

Van ZL, Kimber S, Morris S, Chan KY, Downie A, Rust J et al (2010) Effects of biochar from slow pyrolysis of papermill waste on agronomic performance and soil fertility. Plant Soil 327:235-246

Wan XD, Li Y, Li CY, Xie HJ, Zhang J, Liang S (2020) Effect of iron plaque on the root surface of hydrophyte on nitrogen and phosphorus transformation. Bioresour Technol Rep 12:100566

Wang LY, Qin L, Lv XG, Jiang M, Zou YC (2018) Progress in researches on effect of iron promoting accumulation of soil organic carbon. Acta Pedol Sin 55:1041-1050

Wang MY, Xu XP, Wang WQ, Wang GL, Su CJ, An WL (2017) Effect of slag and biochar amendment on greenhouse gases emissions and related microorganisms in paddy fields. Acta Sci Circumst 37:1046-1056

Wang W, Lai DYF, Li S, Kim PJ, Zeng C, Li P, Liang Y (2014) Steel slag amendment reduces methane emission and increases rice productivity in subtropical paddy fields in China. Wetlands Ecol Manage 22:683-691

Wang W, Lai DYF, Wang C, Tong C, Zeng C (2016) Effects of inorganic amendments, rice cultivars and cultivation methods on greenhouse gas emissions and rice productivity in a subtropical paddy field. Ecol Eng 95:770-778

Wang XT, Xu XP, Wang WQ (2019) Slag and biochar application on community structure and methane emission of iron-reducing bacteria in paddy soil. China Environ Sci 39:2495-2505

Wang YG, Wang HY, Zheng YG, Sun XY (2021) Advances in research methods and control technologies of agricultural non-point source pollution: A review. Chin J Agric Res Reg Planning 42:25-33

Weber KA, Achenbach LA, Coates JD (2006) Microorganisms pumping iron: anaerobic microbial iron oxidation and reduction. Nat Rev Microbiol 4:752-764

Wu C, Qu D, Liu H (2014) Effect of initial pH value on microbial Fe(Ⅲ) reduction in alkaline and acidic paddy soils. Acta Ecol Sin 34:933-942

Wu WJ, Xu YL, Xing SL, Ma FF, Chen NY, Ma YH (2018) Effect of biochar on soil nitrogen and phosphorus transformation and loss. J Agric 8:20-26

Xu M, Gao P, Yang Z, Su L, Wu J, Yang G et al (2019) Biochar impacts on phosphorus cycling in rice ecosystem. Chemosphere 225:311-319

Xu XN (2018) Influences on soil NPK dynamic characteristics and peanut biomass formation by biochar. Liaoning: Shenyang Agricultural University

Xue W (2013) SPSS statistical analysis method and application. Publishing House of Electronics Industry

Yang XJ, Xu Z, Shen H (2018) Drying-submergence alternation enhanced crystalline ratio and varied surface properties of iron plaque on rice (*Oryza sativa*) roots. Environ Sci Pollut Res 25:3571-3587

Yao WQ (2020) Analysis of current situation and countermeasures of agricultural non-point source pollution prevention. Environ Dev 32:42-43

Yu XL, Fu YQ, Gan HH, Shen H (2016) Impacts of drying-wetting cycles on changes of rhizosphere characteristic and the formation of iron plaque: a review. Soils 48:225-234

Zandi P, Yang JJ, Xia X, Krasny BB, Możdżeń K, Puła J et al (2021) Sulphur nutrition and iron plaque formation on roots of rice seedlings and their consequences for immobilisation and uptake of chromium in solution culture. Plant Soil 462:365-388

Zhang QQ, Yan ZZ, Li XZ (2020) Ferrous iron facilitates the formation of iron plaque and enhances the tolerance of *Spartina alterniflora* to artificial sewage stress. Mar Pollut Bull 157:111379

Zhou H, Zhu W, Yang WT, Gu JF, Gao ZX, Chen LW et al (2018) Cadmium uptake, accumulation, and remobilization in iron plaque and rice tissues at different growth stages. Ecotoxicol Environ Saf 152:91-97

Zwieten LV, Kimber S, Morris S, Chan KY, Downie A, Rust J et al (2010) Effects of biochar from slow pyrolysis of papermill waste on agronomic performance and soil fertility. Plant Soil 327:235-246

Figure captions

Fig. 1. Effects of rate of BSF on soil C, N, and P content. All values are mean ± SE (*n* = 3). Different lowercase letters indicate within-growth stage treatment differences and different uppercase letters indicate within-treatment rate differences between growth stages within a season ($p<0.05$).

Fig. 2. Linear regression analysis of soil C, N, and P across all treatments.

Fig. 3. Effects of rate of BSF on soil C, N, and P stoichiometry. All values are mean ± SE (*n* = 3). Different lowercase letters indicate within-growth stage treatment differences and different uppercase letters indicate within-treatment rate differences between growth stages within a season ($p<0.05$).

Fig. 4. Effects of rate of BSF on soil total Fe, ferric Fe, and ferrous Fe concentrations. All values are mean ± SE (*n* = 3). Different lowercase letters indicate within-growth stage treatment differences and different uppercase letters indicate within-treatment rate differences between growth stages within a season ($p<0.05$).

Fig. 5. Effects of rate of BSF on rice root iron plaque content. All values are mean ± SE (n = 3). Different lowercase letters indicate within-growth stage treatment differences and different uppercase letters indicate within-treatment rate differences between growth stages within a season ($p<0.05$).

Fig. 6. Effects of rate of BSF on soil iron-reducing bacteria abundance. All values are mean ± SE (n = 3). Different lowercase letters indicate within-growth stage treatment differences and different uppercase letters indicate within-treatment rate differences between growth stages within a season ($p<0.05$).

Fig. 7. PCA analysis of effects of rate of BSF on soil iron-reducing bacteria community composition at jointing (a) and mature (b) growth stages of early (solid symbols) and late (open symbols) rice. Square: untreated control; circle: 300 kg of BSF ha^{-1}; triangle: 600 kg of BSF ha^{-1}; and, diamond: 900 kg of BSF ha^{-1}.

Fig. 8. Pearson correlation analysis of association between soil physicochemical properties, nutrients, iron metabolism, and iron plaque in early (a) and late (b) rice. Statistical significance is indicated by asterisks: *$p<0.05$, **$p<0.01$ levels. Abbreviations in the figure: WC, water content; BD, bulk density; EC, electrical conductivity; TC, total carbon; TN, total nitrogen; TP, total phosphorus; TFe, total Fe; IRB, iron-reducing bacteria; IP, iron plaque.

Fig. 9. Schematic of iron metabolism and iron plaque formation responses to application of BSF to paddy soils.

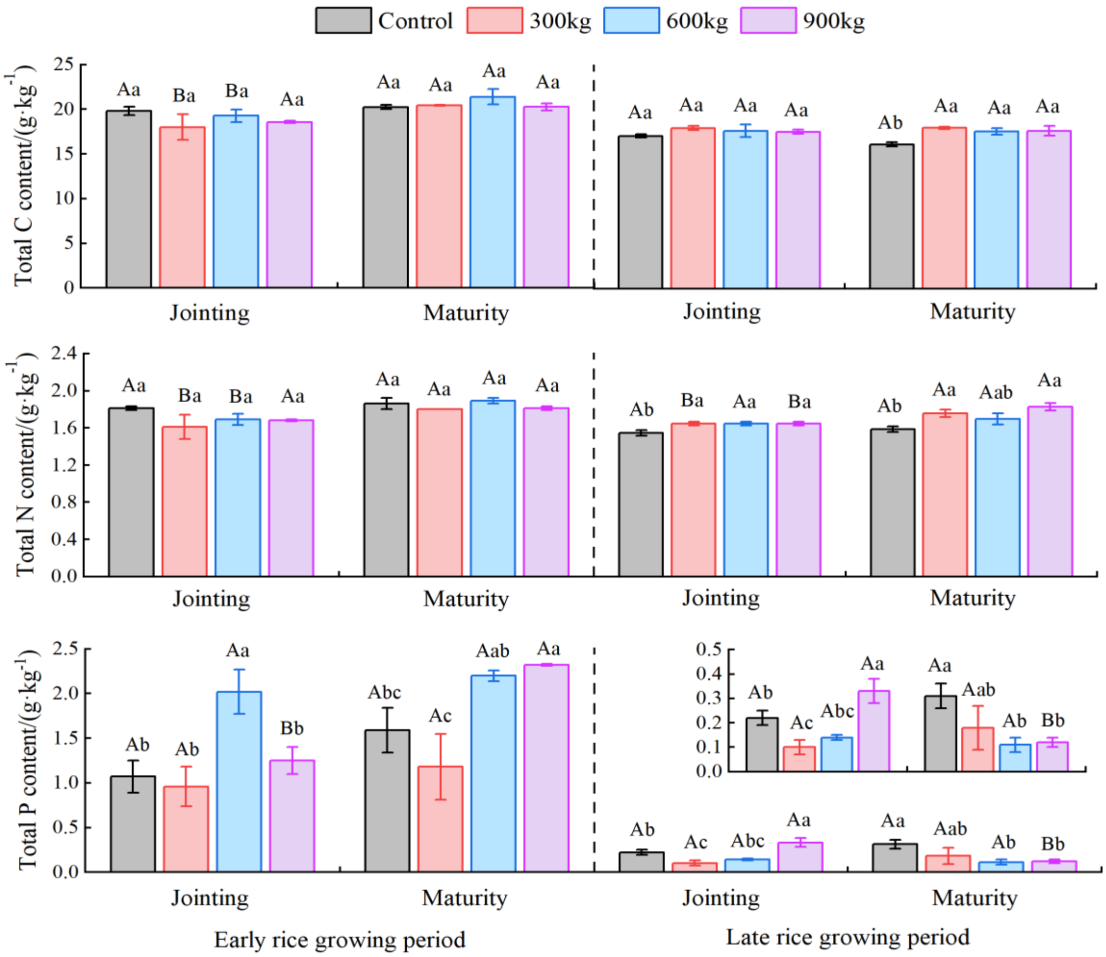

Control
300kg
600kg
900kg
Total C content/(g·kg⁻¹)
Total N content/(g·kg⁻¹)
Total P content/(g·kg⁻¹)
Jointing
Maturity
Early rice growing period
Late rice growing period

Fig. 1.

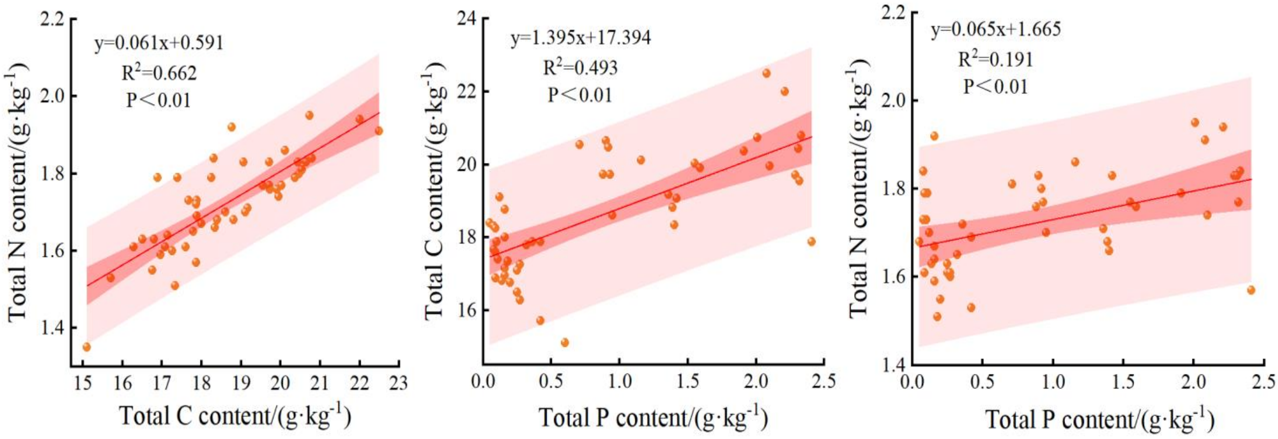
y=0.061x+0.591
R^2=0.662
P<0.01
Total N content/(g·kg^{-1})
Total C content/(g·kg^{-1})
y=1.395x+17.394
R^2=0.493
P<0.01
Total C content/(g·kg^{-1})
Total P content/(g·kg^{-1})
y=0.065x+1.665
R^2=0.191
P<0.01
Total N content/(g·kg^{-1})
Total P content/(g·kg^{-1})

Fig. 2.

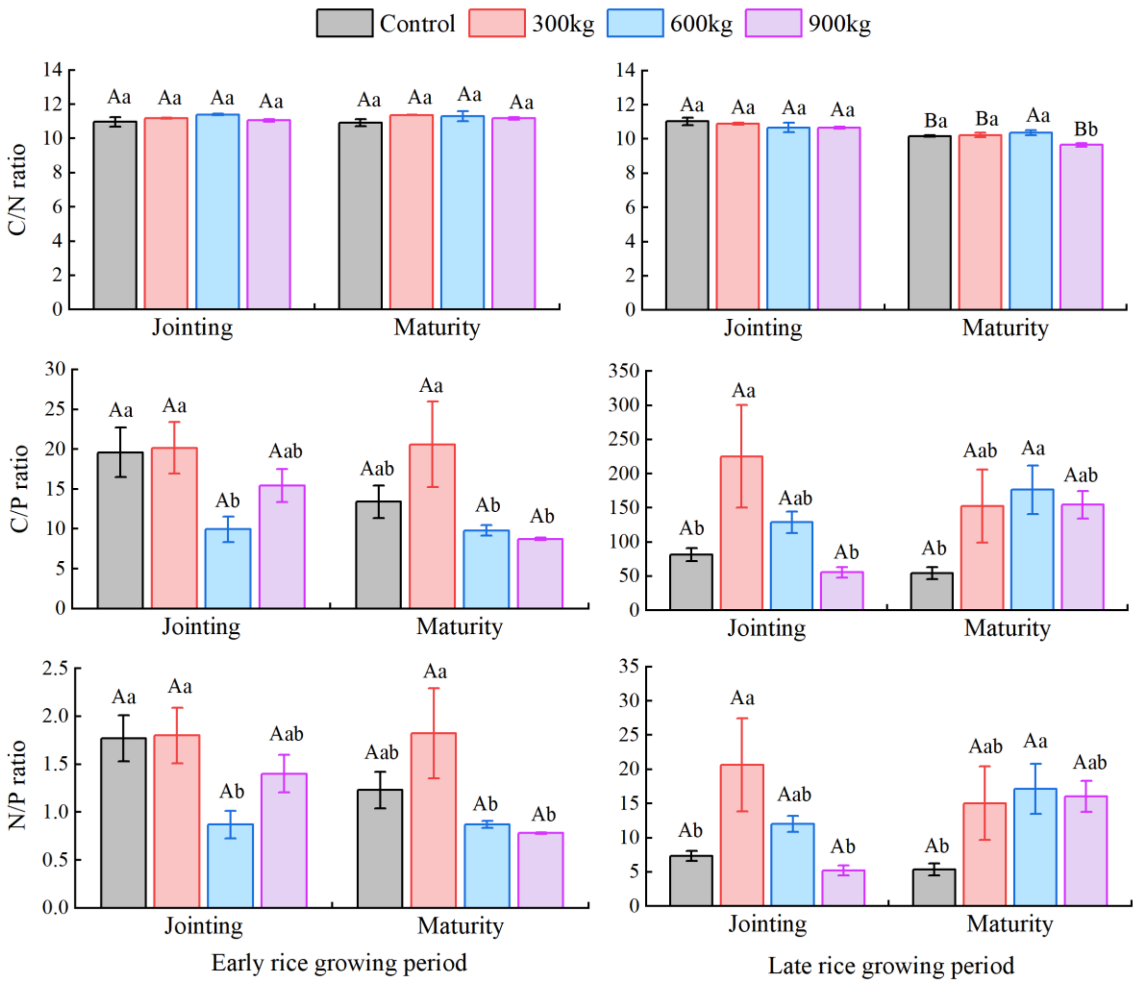
Control
300kg
600kg
900kg
C/N ratio
C/P ratio
N/P ratio
Aa Aa Aa Aa Aa Aa Aa Aa
Aa Aa Aa Aa Ba Ba Aa Bb
Aa Aa Ab Aab Aab Aa Ab Ab
Ab Aa Aab Ab Ab Aab Aa Aab
Aa Aa Ab Aab Aab Aa Ab Ab
Ab Aa Aab Ab Ab Aab Aa Aab
Jointing
Maturity
Early rice growing period
Late rice growing period

Fig. 3.

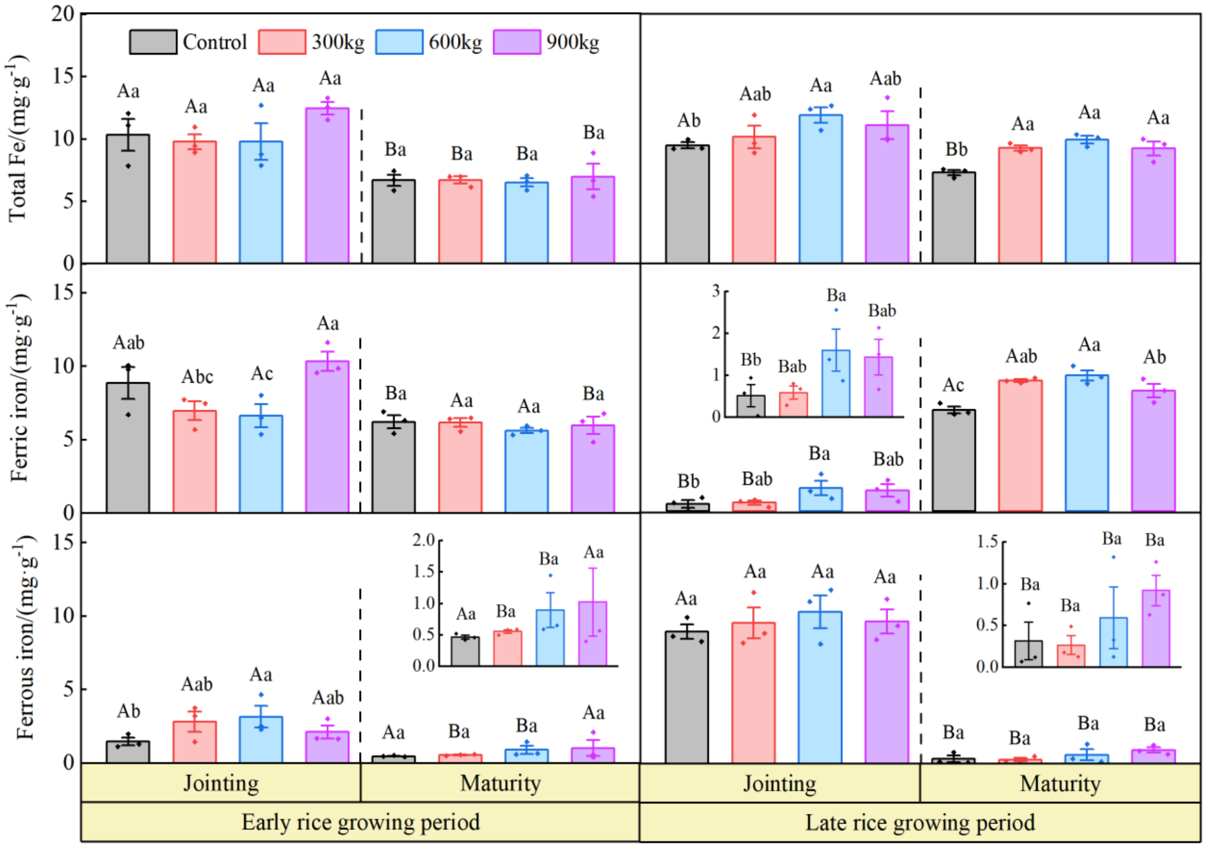
Control
300kg
600kg
900kg
Total Fe/(mg·g⁻¹)
Ferric iron/(mg·g⁻¹)
Ferrous iron/(mg·g⁻¹)
Jointing
Maturity
Jointing
Maturity
Early rice growing period
Late rice growing period

Fig. 4.

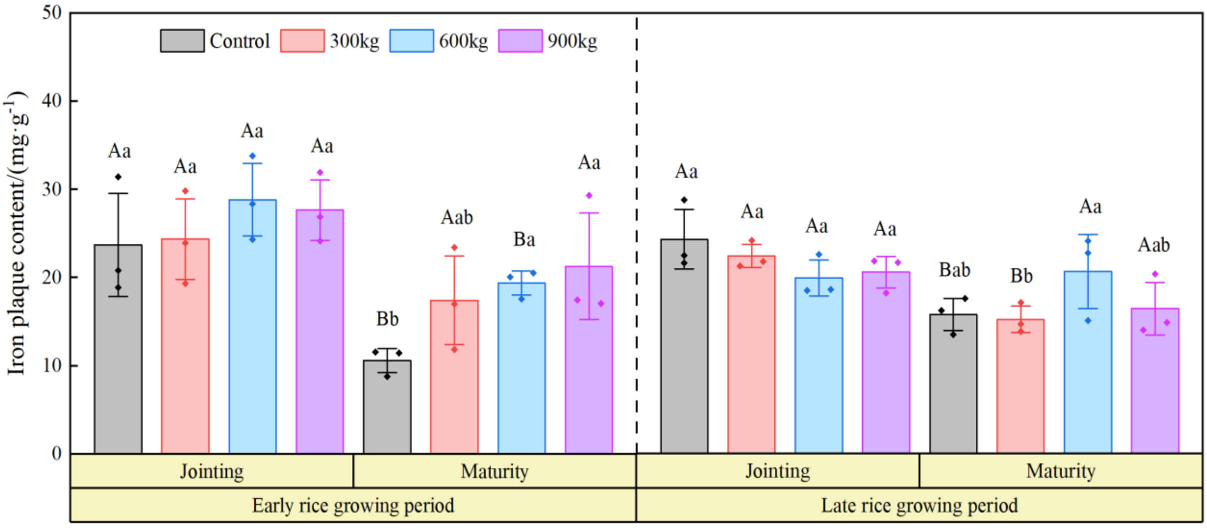
Control
300kg
600kg
900kg
Iron plaque content/(mg·g-1)
50
40
30
20
10
0
Aa
Aa
Aa
Aa
Bb
Aab
Ba
Aa
Aa
Aa
Aa
Aa
Bab
Bb
Aa
Aab
Jointing
Maturity
Jointing
Maturity
Early rice growing period
Late rice growing period

Fig. 5.

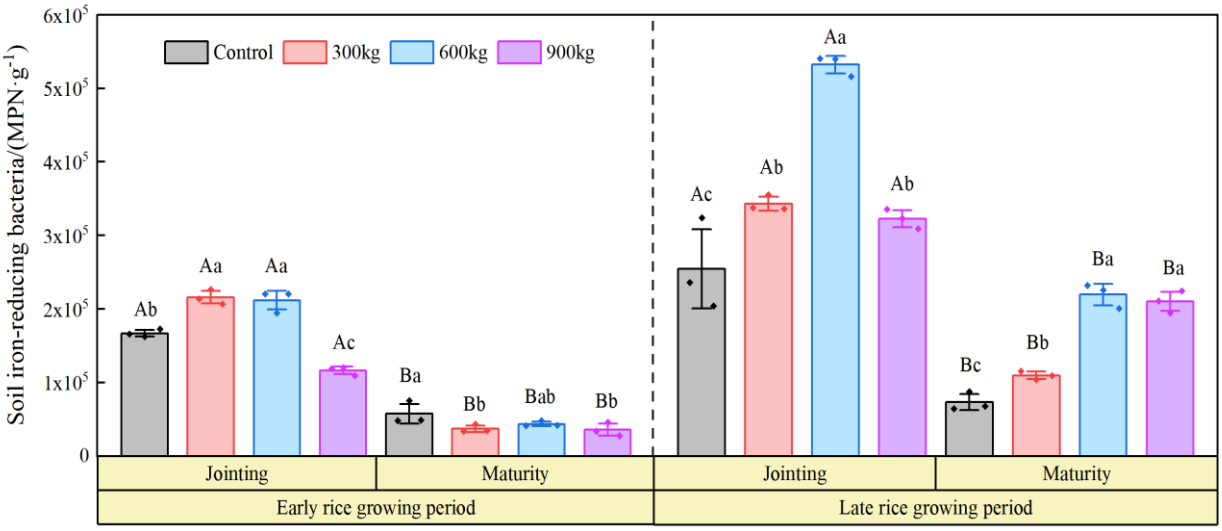
Control
300kg
600kg
900kg
Soil iron-reducing bacteria/(MPN·g⁻¹)
6x10⁵
5x10⁵
4x10⁵
3x10⁵
2x10⁵
1x10⁵
0
Ab
Aa
Aa
Ac
Ba
Bb
Bab
Bb
Ac
Ab
Aa
Ab
Bc
Bb
Ba
Ba
Jointing
Maturity
Jointing
Maturity
Early rice growing period
Late rice growing period

Fig. 6.

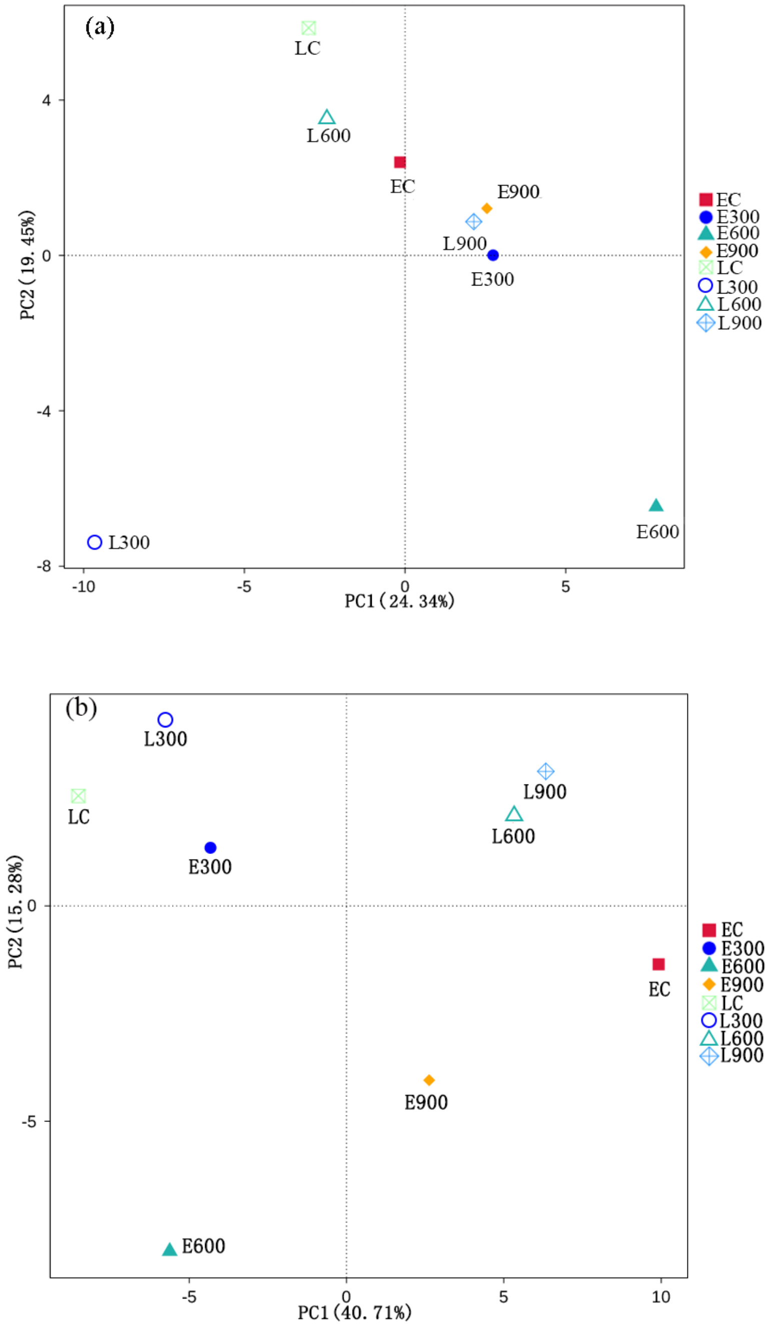
(a)
LC
L600
EC
E900
L900
E300
L300
E600
PC1 (24.34%)
PC2 (19.45%)
4
0
-4
-8
-10
-5
0
5
EC
E300
E600
E900
LC
L300
L600
L900
(b)
L300
LC
E300
L900
L600
EC
E900
E600
PC1 (40.71%)
PC2 (15.28%)
0
-5
-5
0
5
10
EC
E300
E600
E900
LC
L300
L600
L900

Fig. 7.

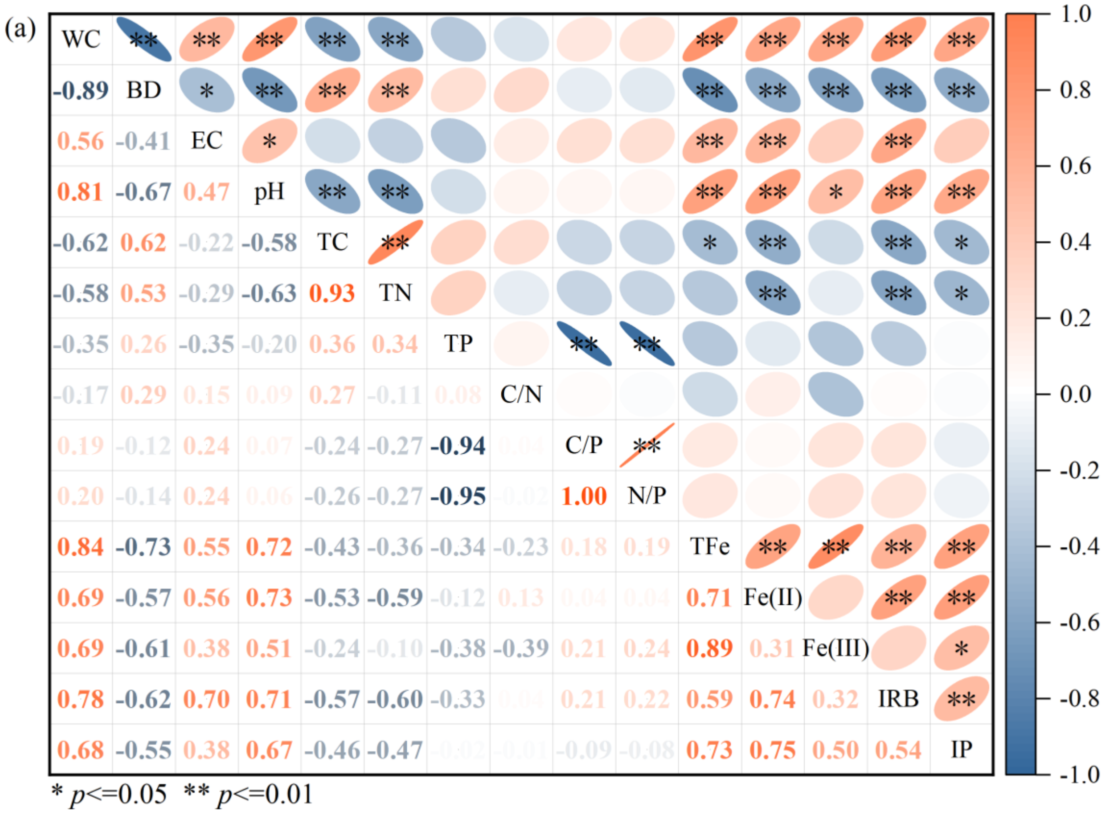
(a)
WC
BD
EC
pH
TC
TN
TP
C/N
C/P
N/P
TFe
Fe(II)
Fe(III)
IRB
IP
1.0
0.8
0.6
0.4
0.2
0.0
-0.2
-0.4
-0.6
-0.8
-1.0
* p<=0.05 ** p<=0.01

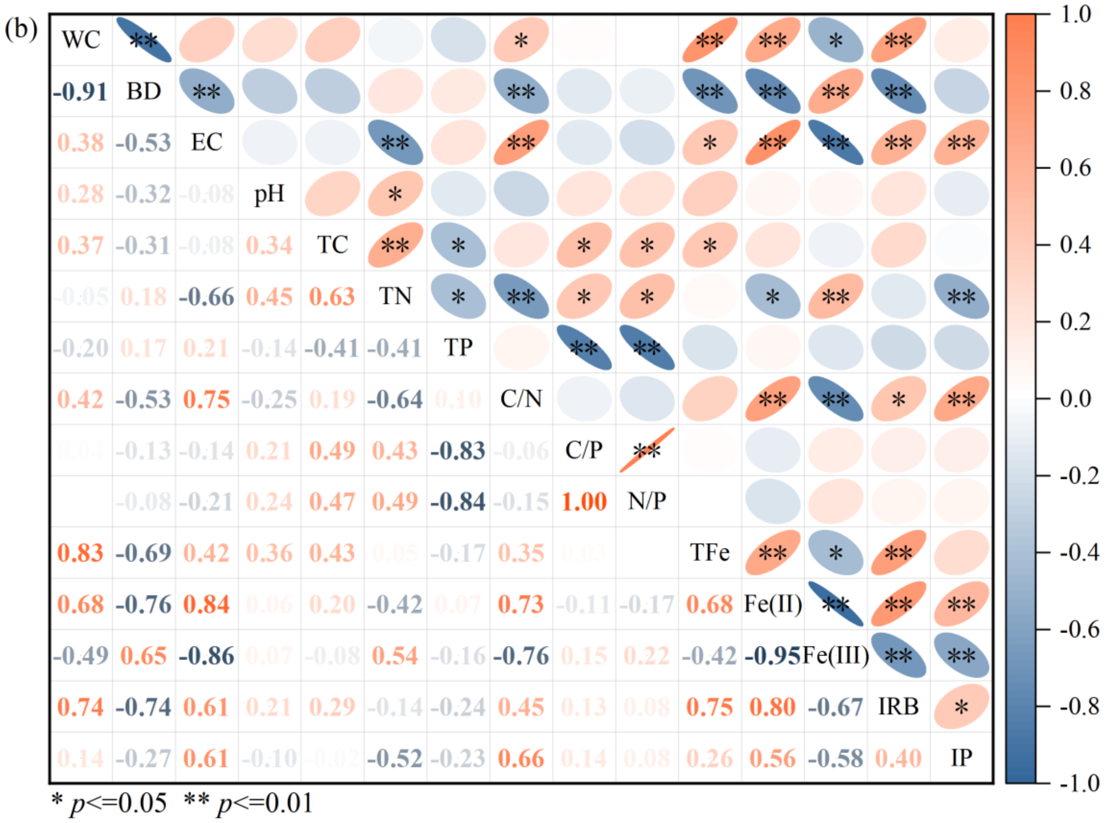
(b)
WC
BD
EC
pH
TC
TN
TP
C/N
C/P
N/P
TFe
Fe(II)
Fe(III)
IRB
IP
1.0
0.8
0.6
0.4
0.2
0.0
-0.2
-0.4
-0.6
-0.8
-1.0
* p<=0.05 ** p<=0.01

Fig. 8.

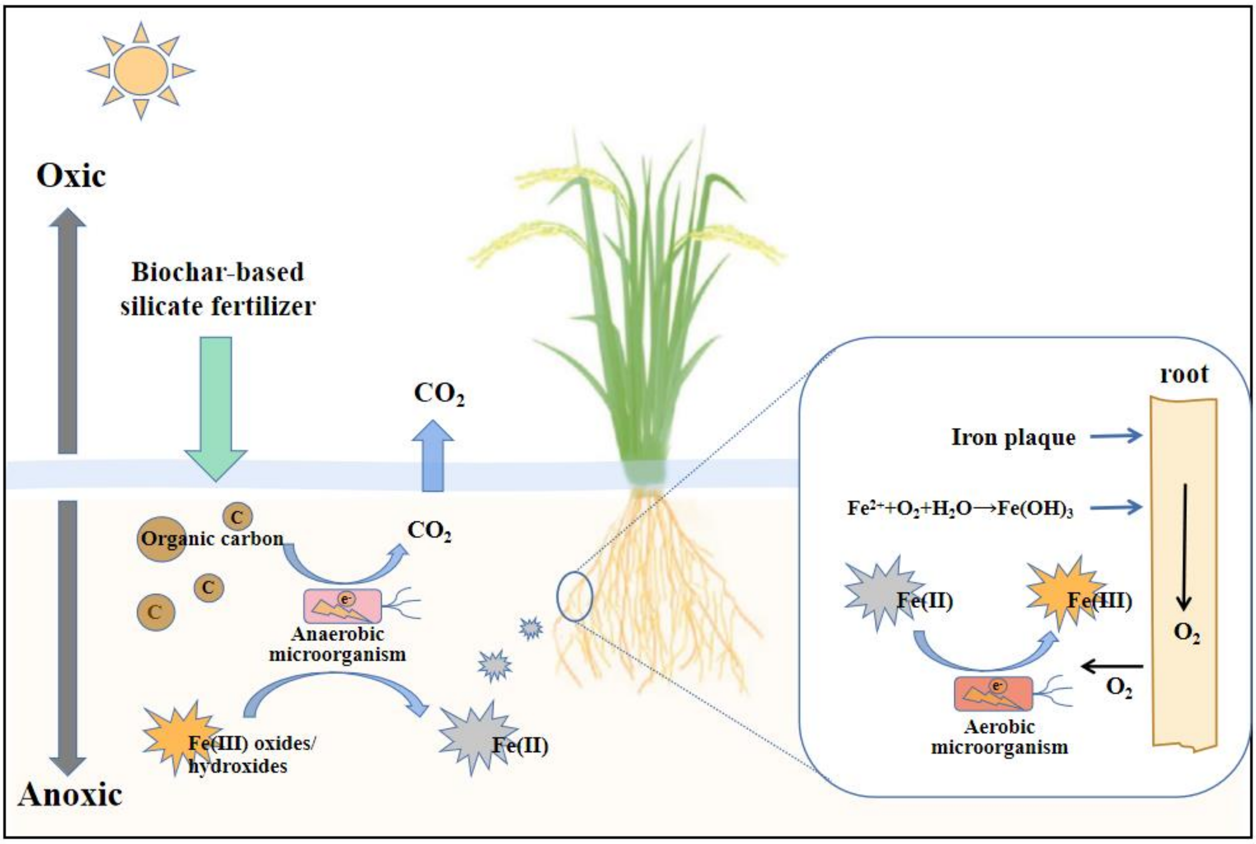
Oxic
Biochar-based silicate fertilizer
CO_2
CO_2
Organic carbon
C
C
C
C
e-
Anaerobic microorganism
Fe(III) oxides/ hydroxides
Fe(II)
Anoxic
root
Iron plaque
$Fe^{2+}+O_2+H_2O \rightarrow Fe(OH)_3$
Fe(II)
Fe(III)
O_2
O_2
e-
Aerobic microorganism

Fig. 9.